Observation of a Reentrant Twist Grain Boundary Phase

D. S. Shankar Rao, S. Krishna Prasad, V. N. Raja, C. V. Yelamaggad, and S. Anitha Nagamani
Centre for Liquid Crystal Research, Jalahalli, Bangalore 560 013, India
(Received 3 April 2001; published 3 August 2001)

We report the occurrence of a reentrant twist grain boundary phase, which we designate as Re-TGB$_A$. Microscopic observations on a nonsymmetric dimer showed the phase sequence Iso–N^*–TGB$_A$–Sm-A–Re–TGB$_A$–TGB$_{C^*}$. Here N^* and Sm-A stand for the chiral nematic and smectic-A phases, TGB$_A$ is the twist grain boundary phase with smectic-A blocks, and TGB$_{C^*}$ that with smectic-C^* blocks and exhibiting features of both the smectic-C^* and TGB phases. The reentrance of the TGB$_A$ phase is unambiguously demonstrated using x-ray diffraction, selective reflection, and optical rotation data.

DOI: 10.1103/PhysRevLett.87.085504 PACS numbers: 61.30.-v, 64.70.Md

A system is said to undergo a "reentrant" phase transition, if a monotonic variation of any thermodynamic field such as temperature or pressure results in two (or sometimes more) phase changes and finally attains a state which is macroscopically similar to the initial state. This phenomenon is exhibited by amazingly diverse condensed matter systems [1]. In liquid crystals such a phenomenon was discovered with the observation of a nematic–Sm-A–reentrant nematic sequence, in the temperature-concentration and temperature-pressure planes [2].

An analogy has been drawn [3] between the N–Sm-A transition and the normal metal-superconductor transition. The analogy is based on the following arguments. In type-I superconducting systems, an applied magnetic field is completely expelled from the superconductor phase, a feature referred to as the Meissner effect. However, in type-II systems, there can be an intermediate phase between the normal phase and the Meissner phase in which the magnetic flux lines penetrate in a regular fashion and form a lattice known as the Abrikosov flux lattice. In liquid crystalline systems, the N^* phase is the analog of a normal metal in an external magnetic field. The expulsion of twist occurring at the N^* to Sm-A transition is then the liquid crystal analog of the Meissner effect. Extending these arguments, Renn and Lubensky [4] postulated a model for the liquid crystal equivalent of a flux lattice phase and referred to it as the twist grain boundary, or TGB, phase. According to the model this phase consists of regularly spaced grain boundaries of screw dislocations, which are parallel to each other within the grain boundary, but are rotated by a finite angle with respect to screw dislocations in adjacent grain boundaries. Independently, experimental observations on a novel Sm-A–like phase reported a helical twist along an axis parallel to the layer planes [5]. Subsequent experiments [6] demonstrated that this phase is indeed the TGB phase. In other words, a macroscopic helix, whose axis is parallel to the layers, is superimposed on blocks of smectic planes. As the layers within each block are Sm-A–like, this phase is referred to as TGB$_A$. Since then theoretical predictions for the existence of TGB$_C$ and TGB$_{C^*}$ phases, with the subscripts indicating the nature of the blocks, have been made [7]. Experimentally, the occurrence of the TGB$_C$ has been well established [8]. More recently, other forms of TGB phases have been experimentally observed, some of whose structure is not yet clear [9,10]. Despite this significant effort on both the experimental and theoretical fronts, the appearance of a reentrant TGB phase has not been theoretically envisaged (for a review, see Kitzerow [9]). On the experimental side, there have been reports [11,12] of the observation of this reentrant phenomenon based on only textural findings without any conclusive proof. In this Letter, we provide the first unambiguous proof for the existence of the reentrant phenomenon for the TGB phase.

The experiments were performed on a cholesterol-based nonsymmetrical dimer, namely, cholesteryl 6-[4-(4-hexyloxy phenylethynyl) phenoxy] hexanoate [13]. We describe observations made under the polarizing microscope using glass plates treated for promoting homeotropic alignment of the molecules. On cooling from the isotropic phase, a focal conic texture appears at 195.2 °C. Slight shearing of the sample leads to a planar texture with oily streaks, a pattern often seen in the chiral nematic phase. By cooling the undisturbed sample, at 154.2 °C, the field of view is filled with a filament texture, which is characteristic of the TGB phase (Fig. 1a). Each filament corresponds to a rotation of the director by π radians, and the width of the filament is equal to half the value of the pitch of the TGB helix. On cooling further, at 145 °C, the filaments vanish leaving the field of view completely dark (Fig. 1b), indicating that the phase could be a Sm-A phase. On lowering the temperature, the filaments reappear (Fig. 1c) at 120 °C, suggesting the existence of another TGB phase. It must be pointed out that in both the high and low temperature TGB phases the filaments were straight without any spatial features. When the sample is cooled below 105 °C the straight filaments develop a spatial periodic modulation (Fig. 1d), a texture which has been recently identified to be characteristic of the TGB$_{C^*}$ phase [9,10] with undulated grain boundaries (see Pramod *et al.* [9]). According to the model proposed by these authors, the blocks are smectic-C^*–like and possess a helix along the smectic layer normal direction, in addition to the usual TGB helix which is parallel to the smectic planes. A particular feature of this model is

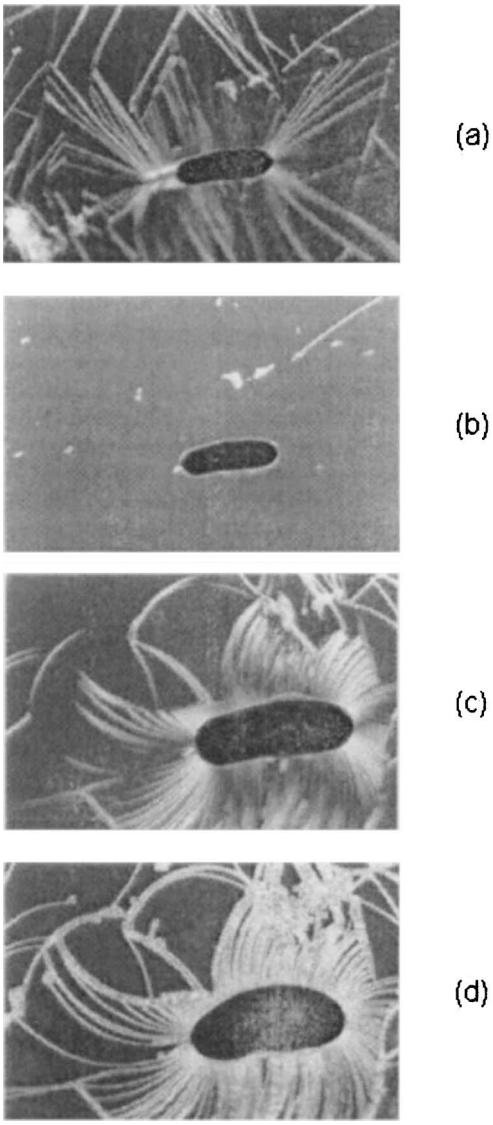

FIG. 1. Photomicrographs taken while cooling the sample from the N^* phase: (a) Filament texture in the high temperature TGB_A phase; the filaments are straight without any spatial modulation. (b) A dark field of view in the Sm-A phase. (c) Reappearance of the filament texture in the Re-TGB_A phase. (d) Filament texture in the TGB_{C^*} phase. Notice the presence of undulation in the filaments and alternate dark and bright bands.

the presence of the undulating grain boundaries. Owing to this undulation the phase is expected to show a square grid pattern when viewed along the TGB helical axis. Indeed our sample showed the square grid pattern in the TGB_{C^*} phase when the observations were done with planar boundary conditions. It may be mentioned that, although not predicted by the standard theories, the TGB_{C^*} has been seen in quite a few materials [10] including a trimesogen, in which it exists over a wide temperature range of 90 °C. From these observations we can give the tentative phase sequence as Iso–N^*–TGB–Sm-A–TGB–TGB_{C^*}. A remark that may be relevant here is that spiral filaments have been seen in the TGB_A phase of a side-chain oligomer; the spiraling effect was due to surface interactions [14]. In contrast, the filaments observed in the TGB_{C^*} phase have a periodic undulation and are argued to be due to the intrinsic helical nature of the Sm-C^* blocks.

To establish the nature of the layering in the high and low temperature TGB phases and the intermediate smectic phase, x-ray diffraction experiments were done. Samples were taken in a Lindemann capillary (1 mm diam.) which was mounted inside a temperature-controlled oven. Diffraction patterns were collected at several temperatures, while cooling the sample from the N^* phase, using an image plate setup [15]. The "one-dimensional trace" taken from typical x-ray diffraction patterns in the N^* and Sm-A phases are shown in Fig. 2. The traces show two sharp low angle reflections, one very intense and the other weak, and a diffuse reflection at wide angles. The spacing of the lowest angle intense peak corresponds to the smectic layer thickness in the Sm-A and the different TGB phases, while in the N^* phase it arises due to the short range layer correlations (the peaks corresponding to this reflection obtained in the different mesophases are shown as an inset in Fig. 2). The diffuse reflection at wide angles has a spacing in the range of 4–5 Å and is associated with the separation between the molecules within the layer. The second peak at low angles is a characteristic feature of dimer molecules [16] and owes its origin to the two individual mesogenic entities which are coupled by a flexible alkylene spacer to form the dimer.

Figure 3 shows the spacing (d) of the lowest angle reflection as a function of temperature. At the transition from the N^* to the TGB phase, a sharp increase in d is seen; it

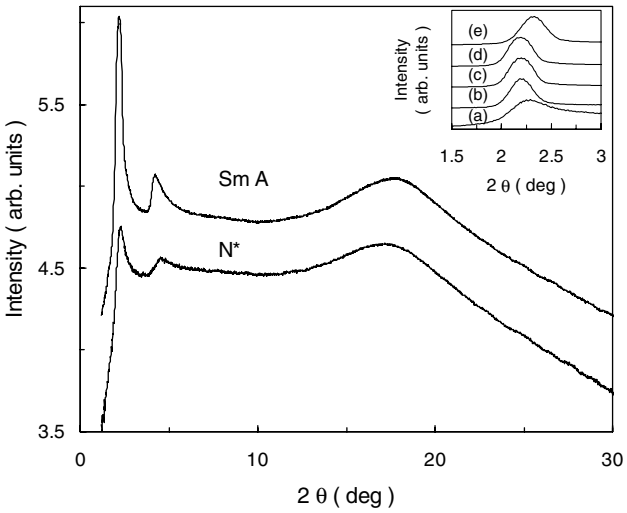

FIG. 2. One-dimensional traces extracted from the x-ray patterns in the N^* and Sm-A phases. Similar traces were obtained for the other mesophases. The lowest angle peak corresponds to the layer thickness in the TGB and Sm-A phases and short range layer correlations in the N^* phase. The second peak at low angles is from the individual mesogenic entities (see text). The wide angle diffuse peak is due to the intermolecular spacing within the layer. The inset shows the evolution of the lowest angle peak in (a) N^*, (b) TGB_A, (c) Sm-A, (d) Re-TGB_A, and (e) TGB_{C^*} phases.

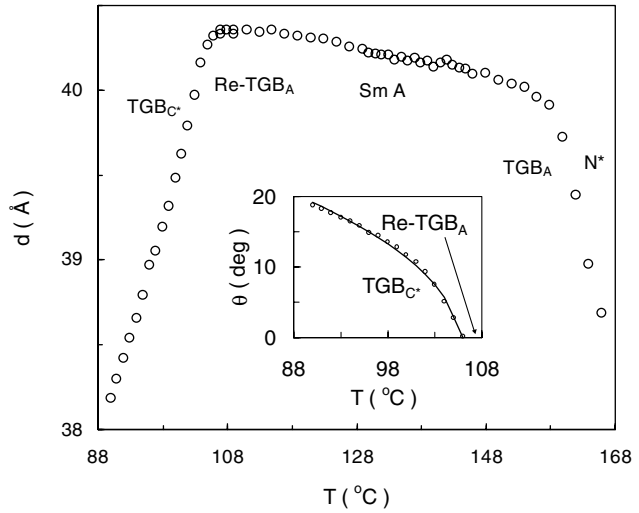

FIG. 3. Plot showing x-ray layer spacing (d) measurements in the Sm-A and the different TGB phases. The values obtained indicate that, except in the TGB$_{C^*}$ phase, $d \sim \ell$ and the molecules are along the layer normal direction. The slight increase with decreasing temperature, before the appearance of the TGB$_{C^*}$ phase, is due to the stretching of the molten aliphatic chains. The onset of the transition to the TGB$_{C^*}$ phase is accompanied by a significant decrease in the value. The magnitude of the decrease is a measure of the tilt angle of the molecules with respect to the layer normal; the temperature variation of the calculated tilt angle θ is shown in the inset. The solid line represents the trend expected by a mean-field model for the Sm-A–Sm-C transition.

was accompanied by an enhancement in the peak intensity, signifying the onset of long range order in layering. The value of d in the TGB phase is comparable to the length, ℓ, of the molecule in its most extended configuration. In fact, the ratio of $d/\ell \sim 0.83$ is typical of the monolayer Sm-A phase or, in this case, blocks of Sm-A layers. Hence, the TGB phase can be identified as a TGB$_A$ phase. The marginal increase in d with decreasing temperature is also a signature of the Sm-A nature of the blocks. This feature, representing a negative thermal expansion due to the stretching of the alkyl chains on lowering the temperature, continues not only in the Sm-A phase but also in the TGB phase which exists just below the Sm-A phase. This behavior in the lower temperature TGB phase is significant, as it identifies the phase also to be a TGB$_A$ phase. The optical studies, described earlier, also showed identical textures in the TGB phases occurring above and below the Sm-A phase. All these features point to the new phenomenon observed, namely, the reentrance of the TGB$_A$ phase. The d value shows a precipitous drop at the transition from the reentrant TGB$_A$ (Re-TGB$_A$) phase to the TGB$_{C^*}$ phase. This is expected, since in the TGB$_{C^*}$ phase the blocks are of the Sm-C^*–type, in which the molecules are tilted with respect to the layer normal direction and therefore the layer thickness will be smaller than in the case where the blocks are of the Sm-A–type. In fact, the tilt angle θ of the molecules in the TGB$_{C^*}$ phase is given by $\theta = \cos^{-1}(d_c/d_A)$, where d_c and d_A stand for the layer spacings in the TGB$_{C^*}$ and TGB$_A$ phases, respectively. To calculate θ, the d_A value is taken as the d value in the Re-TGB$_A$ phase just before the transition to the TGB$_{C^*}$ phase. The temperature variation of θ in the TGB$_{C^*}$ phase is shown in the inset of Fig. 3 and exhibits, as expected, a trend typical of the Sm-C^*–Sm-A transition.

A distinctive feature of the TGB phase is the simultaneous existence of the smectic layering and a helix whose axis is parallel to the layer planes. To demonstrate the existence of such a macroscopic helical structure in the phase just below the Sm-A phase, selective reflection measurements were carried out. For these experiments the sample was contained between glass plates treated to provide planar alignment of the molecules; the cell gap was ~ 30 μm. In this geometry the axis of the TGB helix would be normal to the glass plates, whose pitch value is directly proportional to the wavelength of the selective reflection. A wide band spectrometer (Hitachi model U3400, wavelength range: 180–2500 nm) was used. Typical spectra obtained in the different TGB phases are shown in Fig. 4 (inset). These spectra are characterized by a Bragg reflection band centered at $\lambda_{\min}$, which is related to the pitch, p, of the helical structure by $\lambda_{\min} = pn_{\text{avg}}$; here n_{avg} is the average refractive index of the system. $\lambda_{\min}$ is seen (Fig. 4) to have a weak dependence on temperature far away from the transition to the high temperature TGB$_A$ to Sm-A phase, but diverges on approaching the transition. The most important feature to be noticed is that at a lower temperature it again decreases, having a finite value in the region which has been identified as the Re-TGB$_A$ phase as well as in the TGB$_{C^*}$ phase. Thus, the presence of the macroscopic helix in the direction of

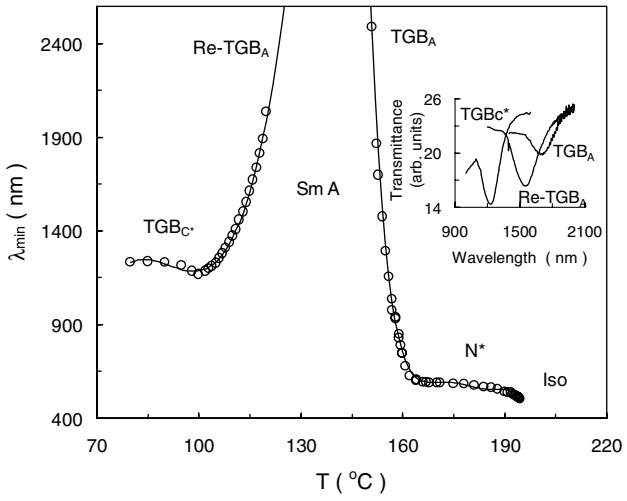

FIG. 4. The inset shows the spectrometer scans obtained in the different TGB phases. The absorption maximum (minimum transmitted light) in each spectrum corresponds to the selective reflection wavelength $\lambda_{\min}$, which is directly proportional to the pitch of the helix. Plot of $\lambda_{\min}$ vs T in the N^* and the TGB phases showing the divergence of $\lambda_{\min}$ as the temperature approaches the transition to the Sm-A phase from both TGB$_A$ and Re-TGB$_A$ phases. The solid line is meant as a guide to the eye.

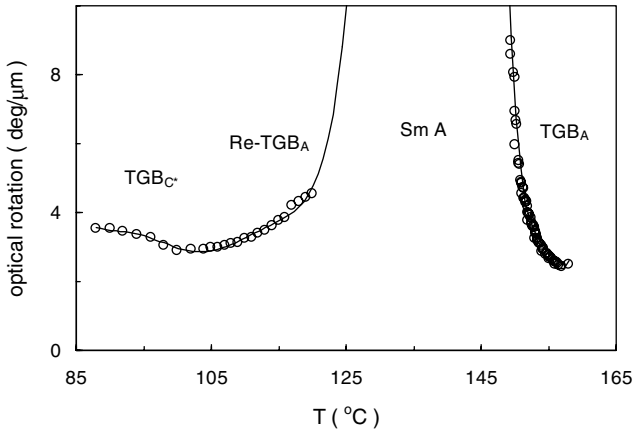

FIG. 5. Thermal variation of the optical rotation of light (wavelength = 633 nm). As seen in the selective reflection measurements, the optical rotation also diverges when approaching the Sm-*A* phase from both TGB$_A$ and Re-TGB$_A$ phases. More importantly, the sense of the rotation remains the same, i.e., positive in the TGB$_A$ phases above and below the Sm-*A* phase, confirming that the TGB$_A$ phase reenters. The solid line is meant as a guide to the eye.

the layer planes, along with the microscopic and x-ray evidence given above, is a clear indication of the existence of the reentrant TGB$_A$ phase. However, it is possible to argue that the optical features seen, namely, microscopic textures, and the trend in the selective reflection data could have been caused by a change in the sense of the rotation of the TGB helix on cooling the sample. In fact, such a change is quite common in the N^* phase and to a lesser extent in the chiral smectic phase [17]. In such a situation, the helical pitch would diverge on approaching the temperature at which the inversion of the sense takes place and would not look very different from the plot shown in Fig. 4. Obviously, in such a case the lower temperature cannot be referred to as a reentrant phase. Therefore, in order to rule out the possiblity of any change in the sense of the helical rotation causing the observed phenomena, we carried out optical rotation studies in the TGB$_A$ and Re-TGB$_A$ phases. The measurements of both the magnitude and sense of the optical rotation were done using a simple polarimeter type of setup, using a He-Ne laser source. The sample geometry was identical to that used for selective reflection experiments.

Figure 5 shows the data collected at several temperatures in the TGB$_A$, Re-TGB$_A$, and TGB$_{C^*}$ phases. The most important point to be noted is that the sense of the rotation remains the same (positive) in all the TGB phases and especially so in the TGB$_A$ and Re-TGB$_A$ phases. The divergence seen on approaching the Sm-*A* phase from both sides is to be expected as there is no macroscopic helical structure in this phase. Of course, owing to the constituting molecules being chiral, there will be a very small optical rotation, whose magnitude is comparable to that observed for all chiral liquids. But this effect is unimportant from the viewpoint of this paper. All the above-mentioned results unequivocally establish the existence of the Re-TGB$_A$ phase.

In summary, we have performed microscopic, x-ray and selective reflection measurements on a dimer liquid crystal and clearly demonstrate the existence of a reentrant twist grain boundary phase.

We are indebted to Professor S. Chandrasekhar for his keen interest in this work and several useful discussions. Our thanks are due to Dr. Geetha G. Nair for her help in the experiments and active participation in the discussions.

[1] T. Narayanan and A. Kumar, Phys. Rep. **249**, 135 (1994).
[2] For a review, see, P. E. Cladis in *Physical Properties of Liquid Crystals,* edited by D. Demus *et al.* (Wiley VCH, Weinheim, 1999).
[3] P. G. de Gennes, Solid State Commun. **10**, 753 (1972).
[4] S. R. Renn and T. C. Lubensky, Phys. Rev. A **38**, 2132 (1988).
[5] J. W. Goodby *et al.,* Nature (London) **337**, 449 (1989).
[6] G. Srajer *et al.,* Phys. Rev. Lett. **64**, 1545 (1990).
[7] S. R. Renn, Phys. Rev. A **45**, 953 (1992).
[8] L. Navailles, P. Barois, and H. T. Nguyen, Phys. Rev. Lett. **71**, 545 (1993).
[9] W. Kuczynski and H. Stegemeyer, Mol. Cryst. Liq. Cryst. **260**, 377 (1995); Proc. SPIE Int. Soc. Opt. Eng. **3318**, 90 (1997); P. A. Pramod, R. Pratibha, and N. V. Madhusudana, Curr. Sci. **73**, 761 (1997); G. G. Nair, Curr. Sci. **74**, 98 (1998); A. C. Ribeiro *et al.,* Eur. Phys. J. B **11**, 121 (1999); J. C. Meier *et al.,* in Proceedings of the 18th ILCC, Sendai, Japan, 2000, Abstract No. 26E-22-P (to be published); for reviews, see J. W. Goodby, in *Structure and Bonding, Liquid Crystals II,* edited by D. M. P. Mingos (Springer-Verlag, Berlin, 1999); H. S. Kitzerow, in *Chirality in Liquid Crystals,* edited by H. S. Kitzerow and C. Bahr (Springer-Verlag, New York, 2001).
[10] C. V. Yelamaggad *et al.,* J. Chem. Soc. Chem. Commun. **2000**, 57.
[11] V. Vill and H. W. Tunger, J. Chem. Soc. Chem. Commun. **1995**, 1047.
[12] V. Vill, H. W. Tunger, and D. Peters, Liq. Cryst. **20**, 547 (1996).
[13] C. V. Yelamaggad *et al.* (to be published). The purity of the sample, as well as its molecular structure, has been evidenced with the help of spectroscopic (^{1}H, ^{13}C NMR, and mass spectroscopy) analyses. Elemental analysis was found to be consistent with the proposed structure of the compound.
[14] J. M. Gilli and M. Kamaye, Liq. Cryst. **12**, 545 (1992).
[15] Sandeep Kumar, D. S. Shankar Rao, and S. Krishna Prasad, J. Mater. Chem. **9**, 2751 (1999).
[16] F. Hardouin *et al.,* J. Phys. II (France) **4**, 627 (1994).
[17] A. J. Slaney *et al.,* J. Mater. Chem. **2**, 805 (1992); J. W. Goodby *et al.,* Ferroelectrics **147**, 291 (1993); I. Dierking *et al.,* Z. Naturforsch A **49**, 1081 (1994); M. Kaspar *et al.,* Liq. Cryst. **19**, 589 (1995); V. Vill *et al.,* Liq. Cryst. **20**, 449 (1996).